Dynamic control of the photonic stop bands formed by a standing wave in inhomogeneous broadening solids

Qiong-Yi He,[1,2] Jin-Hui Wu,[1,2] Tie-Jun Wang,[1,2] and Jin-Yue Gao[1,2,*]

[1]*College of Physics, Jilin University, Changchun 130023, People's Republic of China*

[2]*Key lab of Coherent Light, Atomic and Molecular Spectroscopy, Educational Ministry of China,*
Changchun, People's Republic of China

When a three-level system is coherently driven by a strong modified standing wave, photonic band gaps are viable to realize. Theoretically detailed calculations, for Pr^{3+}-doped yttrium orthosilicate crystal with inhomogeneously broadening, further show that the gap structure can be dynamically controlled and optimized by modulating the Rabi frequency, the spatial periodicity of the standing wave, the reflectivity of mirror, and the angle of incidence. This adjustable photonic band gap determined by the external pump control parameters in a doped solid crystal should hold more potential for applications than that in typical photonic crystals which are determined once for all by the way the material periodic structure is grown.

PACS number(s): 42.50.Gy, 03.75.Be, 42.30.Rx

I. INTRODUCTION

Quantum coherence and interference in an optical medium interacting with radiation fields have been extensively studied both experimentally and theoretically. Many fascinating phenomena have been revealed and discussed, among which the most typical one is electromagnetically induced transparency (EIT) [1,2]. In recent years, EIT in solid media with inhomogeneous broadening and related phenomena have been studied more and more extensively [3–8]. In particular, a standard Λ configuration for EIT produced by a driving standing wave control beam has currently attracted the great attention of both theorists and experimentalists [9–11]. Few theoretical works were devoted on the investigation that probe propagation can be modulated periodically in space via controlled modification of the photonic density of states in EIT media by periodic modulating the refractivity index with a modified standing wave (SW-EIT), which can realize a photonic band gap (PBG) [12–14].

The proposed PBG has potential applications for the dynamic control of group velocity, dispersion compensation in fiber-optic communications. In a standard PBG system, the spatial dependence of the optical response and the corresponding photonic band structure are determined once and for all by its material composition, i.e., its structure. It is, however, of great interest for the possibility to tune the PBG properties in a fast and efficient way without changing the material structure itself. Now, a suitable mechanism to achieve very large modulations of the optical properties can be realized in SW-EIT photonic crystals via quantum coherence and interference in a multilevel system [12–14].

The purpose of this paper is to extend the above studies from cold atomic [14] to inhomogeneous broadening doped solids. Here by studying for Pr^{3+}-doped yttrium orthosilicate (Pr: YSO), we show that the PBG in a doped solid SW-EIT photonic crystal can be dynamically controlled and opti-

mized by the following factors: the Rabi frequency; the standing wave periodicity; the reflectivity of mirror; and the angle of incidence. We analyze the physical mechanism of these factors in detail by a comparison between standard photonic crystals and SW-EIT photonic crystals. This process enables one to control a PBG with facility dynamically that are impossible with conventional photonic crystal materials. Such photonic media are sought after as a promising avenue, e.g., toward deterministic photon-photon entanglement [15] or the enhancement of nonlinear interactions between weak light pulses [16].

II. THE MODEL AND EQUATIONS

We consider a simplified three-level Λ system shown in Fig. 1. The energy-level scheme is relevant to the case Pr^{3+}-doped yttrium orthosilicate (Pr: YSO) crystal, where levels $|b\rangle$, $|c\rangle$, and $|a\rangle$ correspond to energy levels of Pr^{3+} ions $^3H_4$ ($\pm 3/2$), $^3H_4$ ($\pm 1/2$), $^1D_2$ ($\pm 1/2$), respectively. Levels $|a\rangle$ and $|b\rangle$ are coupled by a weak probe beam with frequency ω_p, the transmission of which are the physical quantities we are interested in. Between levels $|a\rangle$ and $|c\rangle$, a standing wave (SW) pattern created by a strong coupling
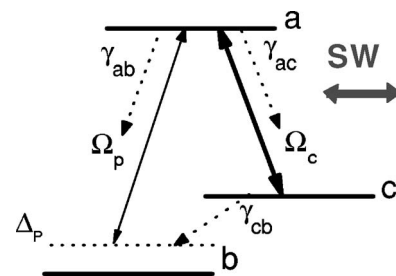

FIG. 1. Three-level Λ model for electromagnetically induced transparency. The probe (signal) field is nearly resonant with the transition from the ground state $|b\rangle$ to the excited state $|a\rangle$ and the control fields (standing wave) is tuned at resonance between $|c\rangle$ and $|a\rangle$.

*Electronic mail: jygao@mail.jlu.edu.cn

TABLE I. Relevant experimental parameters [4].

Case	W^{ab} (MHz)	W^{cb} (KHz)	Γ_{ab} (KHz)	γ_{ab} (KHz)	Γ_{cb} (Hz)	γ_{cb} (KHz)	λ (nm)	f	N (cm^{-3})
Pr: YSO	1	30	6.098	9.009	0.01	2	605.7	3×10^{-7}	1.17×10^{15}

fields at frequency ω_c with Rabi frequency of Ω_0 and its reflection manipulates the probe propagation via induced refractive index change of the medium. The control beam is retroreflected along the x direction upon impinging on a mirror of reflectivity R_m. Thus, the resulting pump Rabi frequency varies periodically along x

$$\Omega_C^2(x) = \Omega_0^2 \left[(1 + \sqrt{R_m})^2 \cos^2\left(\frac{\omega_c}{c} x\right) \right. $$
$$\left. + (1 - \sqrt{R_m})^2 \sin^2\left(\frac{\omega_c}{c} x\right) \right], \quad (1)$$

with a spatial periodicity a equals $\lambda_c/2$. The tunable parameter $\eta = (1 - \sqrt{R_m})/(1 + \sqrt{R_m})$ $(0 \leq \eta < 1)$ is introduced in Ref. [14]. For $\eta = 0$, it is a perfect standing wave. By slightly reducing the mirror reflectivity ($\eta \neq 0$), the nodes of the standing wave will be replaced by quasinodes.

Based on the semiclassical theory, using the standard density matrix formalism with the dipole approximation and the rotating wave approximation, the interaction Hamiltonian H_1 for this system is ($\hbar = 1$)

$$H_I = \Delta_P |a\rangle\langle a| - (\Omega_p |a\rangle\langle b| + \Omega_c |a\rangle\langle c| + \text{H.c.}), \quad (2)$$

where the detunings of the probe field and the coherent driving field are defined as Δ_p and Δ_c. Here we assume $\Delta_c = 0$. The Rabi frequency of the probe field is defined as $\Omega p = \mu_{ab} E_p / 2\hbar$, where μ_{ab} represents the matrix element of the dipole moment between levels $|a\rangle$ and $|b\rangle$.

Then we obtain the equations of motion for the density operators in the interaction picture, (here the Rabi frequencies are assumed to be real)

$$\dot{\rho}_{aa} = -(\Gamma_{ab} + \Gamma_{ac})\rho_{aa} - i\Omega_p(\rho_{ab} - \rho_{ba}) - i\Omega_c(\rho_{ac} - \rho_{ca}),$$

$$\dot{\rho}_{bb} = \Gamma_{ab}\rho_{aa} + \Gamma_{cb}\rho_{cc} - \Gamma_{bc}\rho_{bb} + i\Omega_p(\rho_{ab} - \rho_{ba}),$$

$$\dot{\rho}_{cc} = \Gamma_{ac}\rho_{aa} - \Gamma_{cb}\rho_{cc} + \Gamma_{bc}\rho_{bb} + i\Omega_c(\rho_{ac} - \rho_{ca}),$$

$$\dot{\rho}_{ab} = -(i\Delta_{ab} + \gamma_{ab})\rho_{ab} - i\Omega_p(\rho_{aa} - \rho_{bb}) + i\Omega_c\rho_{cb},$$

$$\dot{\rho}_{cb} = -(i\Delta_{cb} + \gamma_{cb})\rho_{cb} - i\Omega_p\rho_{ca} + i\Omega_c\rho_{ab},$$

$$\dot{\rho}_{ac} = -(i\Delta_{ac} + \gamma_{ac})\rho_{ac} + i\Omega_p\rho_{bc} - i\Omega_c(\rho_{aa} - \rho_{cc}),$$

$$1 = \rho_{aa} + \rho_{bb} + \rho_{cc},$$

$$\rho_{ij} = \rho_{ji}^*. \quad (3)$$

Where Γ_{ij} ($i, j = a, b, c$) are the population relaxation rates. We take $\Gamma_{cb} = \Gamma_{bc}$ so that before the action of the drive field the levels $|b\rangle$ and $|c\rangle$ are equally populated. The coherence

decay rates for ρ_{ab}, ρ_{ac}, and ρ_{cb} are denoted by γ_{ab} γ_{ac}, and γ_{cb}, respectively. We assume that $\gamma_{ab} = \gamma_{ac} = \gamma$. The Δ_{ij} are given by $\Delta_{ab} = \omega_{ab} - \omega_p = \Delta_p + \Delta\omega_{ab}$, $\Delta_{ac} = \omega_{ac} - \omega_c = \Delta\omega_{ac}$, $\Delta_{cb} = \omega_{cb} - \omega_p + \omega_c = \Delta_p + \Delta\omega_{cb}$, and $\Delta\omega_{ac} = \Delta\omega_{ab} - \Delta\omega_{cb}$. Here ω_{ab}, ω_{ac}, and ω_{cb} are the frequencies of the corresponding transitions, while $\Delta\omega_{ij}$ represents the detuning of the inhomogeneous broadened line center from an isolated atom line center.

In the presence of the pump field, the steady state solution ρ_{ab} can be found to the first order in the probe field, from which the dressed susceptibility seen by the probe is obtained.

However, the analysis above yields the relevant equations for a single atom with specific detuning defined by its position within its host only. In order to obtain the relevant macroscopic susceptibility χ, such result has to be averaged over the entire frequency range of the corresponding transitions, as determined by the inhomogeneous broadening of the impurity lines in the host solid. We hereafter follow the treatment of Ref. [17], assuming that the inhomogeneous broadening could be described by a Lorentzian, and obtain [18]

$$\chi(\omega) = \int d(\omega_{ab}) f(\omega_{ab}) \int d(\omega_{cb}) f(\omega_{cb}) \left(\frac{N\mu_{ab}^2}{2\hbar} \frac{\rho_{ab}}{\Omega_p} \right), \quad (4)$$

$$f(\omega_{ab(cb)}) = \frac{W^{ab(cb)}/\pi}{(\Delta\omega_{ab(cb)})^2 + (W^{ab(cb)})^2}, \quad (5)$$

where W^{ab}, W^{cb} are the inhomogeneous widths of the transitions $|a\rangle \rightarrow |b\rangle$ and $|c\rangle \rightarrow |b\rangle$, respectively, and N is the number of optically relevant impurities per unit volume. Finally, the dressed dielectric function experienced by the probe can be written as

$$\varepsilon(\omega) = n^2(\omega) = 1 + 4\pi\chi(\omega). \quad (6)$$

Owing to the spatially periodic modulation induced by the pump, the probe propagates in the coherently dressed system described by Eqs. (1)–(6) as in a one-dimensional photonic crystal and, because of $\omega_p \approx \omega_{ab}$, the probe wave vector is close to the corresponding Brillouin zone boundary (π/a) and the opening of a photonic stop band can be anticipated [14]. As the first step to obtain the photonic band structure of the probe, a 2×2 unimodular transfer matrix [19] $M(\omega)$ representing the propagating through a single period is calculated numerically [13]. Then, the translational invariance of the periodic medium is fulfilled by imposing the Bloch condition [20] on the photonic eigenstates
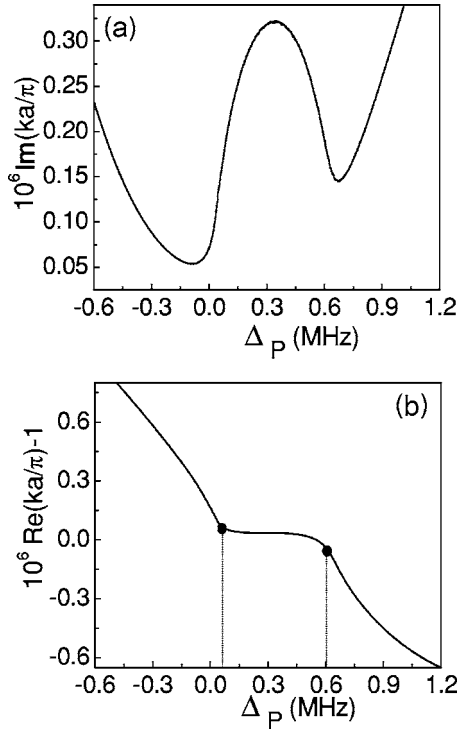
FIG. 2. Photonic band-gap structure near the Brillouin zone boundary in Pr: YSO when $\Omega_0 = 10$ MHz, $\eta = 0.05$, and $\alpha = 0.98$ mrad. (a) and (b) frames denote, respectively, the imaginary and real parts of the Bloch wave vector.

$$\begin{pmatrix} E^+(x+a) \\ E^-(x+a) \end{pmatrix} = M(\omega) \begin{pmatrix} E^+(x) \\ E^-(x) \end{pmatrix} = \begin{pmatrix} e^{i\kappa a} E^+(x) \\ e^{i\kappa a} E^-(x) \end{pmatrix}, \quad (7)$$

where E^+ and E^- are the electric field amplitudes of the forward and backward (Bragg reflected) propagating probe, respectively. κ is the Bloch wave vector of the corresponding probe photonic state ($\kappa = \kappa' + i\kappa''$ is complex in general). The one-dimensional photonic band structure is obtained from the solution of the corresponding determinantal equation $e^{2i\kappa a} - \text{Tr}[M(\omega)]e^{i\kappa a} + 1 = 0$ (det $M = 1$), and noting that if κ is a solution, $-\kappa$ is a solution, too. One simply has [13]

$$\kappa a = \pm \cos^{-1}\left[\frac{\text{Tr}[M(\omega)]}{2} \right]. \quad (8)$$

As previous work introduced in Refs. [13,14], it is necessary to consider a finite sample of thickness $L = Na$ ($N \gg 1$) where N is the number of the standing wave periods. The total transfer matrix $M_{(N)}$ of a sample with thickness L is simply given in terms of the single period transfer matrix M as $M_{(N)} = M^N$. Because M is unimodular, the following closed expression for $M_{(N)}$ holds true:

$$M_{(N)} = \frac{\sin(N\kappa a)}{\sin(\kappa a)} M - \frac{\sin[(N-1)\kappa a]}{\sin(\kappa a)} I, \quad (9)$$

where I is the unity matrix. Such a compact expression enables one to write the reflection (R_N) and transmission (T_N) amplitudes for the L length in terms of complex Bloch wavevector κ and the elements M_{ij} of the matrix M, namely,

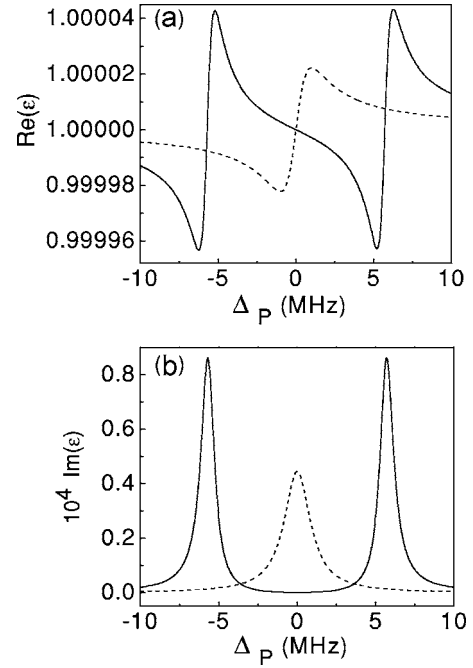FIG. 3. Real (a) and imaginary (b) part of the dressed dielectric function for Pr: YSO when $\Omega_c = 3$ MHz (solid lines) and $\Omega_c = 0$ MHz (dashed lines).

$$R_N = \frac{M_{N(12)}}{M_{N(22)}} = \frac{M_{12}\sin(N\kappa a)}{M_{22}\sin(N\kappa a) - \sin[(N-1)\kappa a]}, \quad (10)$$

$$T_N = \frac{1}{M_{N(22)}} = \frac{\sin(\kappa a)}{M_{22}\sin(N\kappa a) - \sin[(N-1)\kappa a]}, \quad (11)$$

from which, the reflectivity, transmissivity, and absorption can be found by calculating $|R_N|^2$, $|T_N|^2$, and $A = 1 - |R_N|^2 - |T_N|^2$, respectively.

III. NUMERICAL RESULTS AND DISCUSSION

By using the above formulas and solution of the probe propagation developed in the previous section, we can perform numerical calculations to show the effect of various factors on PBG in the case of experimental interest [3], Pr: YSO, in which EIT has been already observed [4]. All relevant experimental parameters are listed in Table I. Here we should note the inhomogeneous broadening can be reduced to the magnitude of the laser beam jitter ($\Delta \nu_{jit} = 1$ MHz) using an optical repump scheme, at the price of reducing the effective density of Pr ions to 1.17×10^{15} cm^{-3} [4].

Figure 2 shows the photonic band gap structure around the lowest photonic band gap that has been studied in our previous work [21]. Here $\eta = 0.05$ and then Rm$= 0.905$, so by the formula (1) the pump Rabi frequency have the smallest value $\Omega c\_\text{min} = 0.308\Omega_0 \approx 3$ MHz at the quasinodes, and the largest value $\Omega c\_\text{max} = 1.38\Omega_0 \approx 13$ MHz at antinodes. In Fig. 3 it is clear that the EIT linewidth is about equal to 5 MHz when pump Rabi frequency is about equal to the smallest value. So EIT also exists at the quasinodes, and the
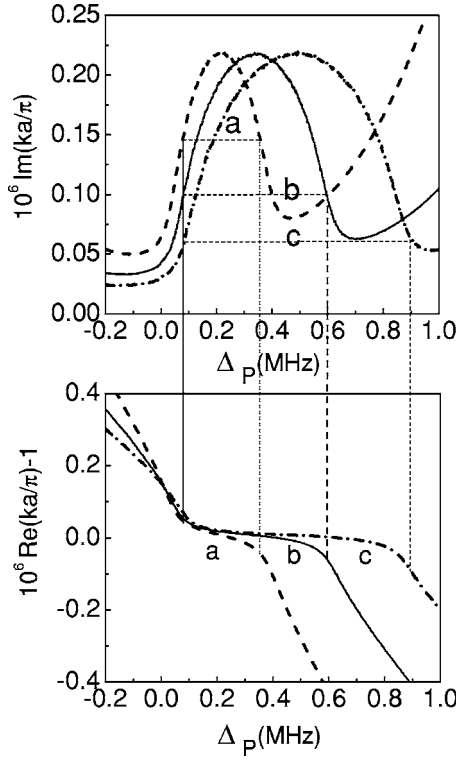
FIG. 4. Probe photonic band structure near the Brillouin zone boundary when a modified SW pump with $\alpha=0.98$ mrad and $\eta=0.1$ is on, corresponds to different Rabi frequencies: $\Omega_{0(a)}=8$ MHz, $\Omega_{0(b)}=10$ MHz, $\Omega_{0(c)}=12$ MHz.
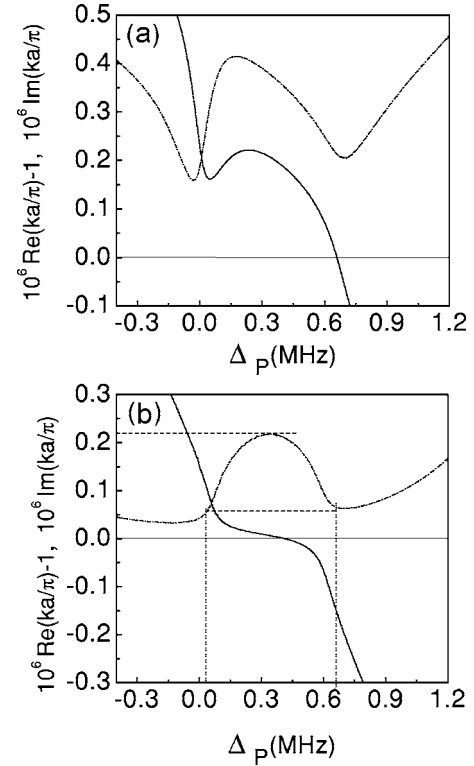

FIG. 5. Band-gap structure near the Brillouin zone boundary when a modified SW pump with $\alpha=0.98$ mrad and (a) $\eta=0$, (b) $\eta=0.1$ is on. Both real (solid) and imaginary (dash) parts of the Bloch wave vector are shown. The pump intensity of the two case is $\Omega_0=10$ MHz.

narrow band gap is all contained within the transparency window.

In the standard photonic crystals, it is well known that the periodic arrangement of refractive index variation controls how photons to move through the crystal [22]. The relative width of the band gap will get wider with the increment of the smaller and larger refractive index ratios in one period [23,24]. Accordingly, a natural question that arises is whether there exists a factor, which controls the width of PBG in the model under investigation. By Eqs. (3), (4), and (6), we can find that the refractive index ratio is related to the Rabi frequency of standing wave pump. So, we can anticipate that the width of the band gap will increase with the increment of the intensity enhancement of SW Rabi frequency. The theoretical studies may indicate that the answer to this question is positive for Pr: YSO, which is shown in Fig. 4.

At the same time, from this figure, one also can find that within the gap edges κ'' is reduced with the increasing of gap width, where the corresponding reflection must be reduced. This may be understood by noticing that the larger Rabi frequency must conduce to the wider EIT linewidth. As the consequence, the transmission will be strengthened, i.e., more section of probe will transmit the medium. Therefore, in order to get the better band gap for the lights that we want to forbid them to propagate; we need to counterpoise the two effects of the pump Rabi frequency.

Next we consider the function of tunable parameter η and the misalignment α, while keeping pump Rabi frequency. It can be found from Fig. 5(a) that the band gap in the first

Brillouin zone boundary is barely defined for $\eta=0$, but when we slightly change η, a well-developed band gap characterized by $\kappa' \approx \pi/a$ and $\kappa'' \neq 0$ appears as shown in Fig. 5(b). The explanation to this phenomenon is likely to the EIT disappears at the nodes of standing wave for $\eta=0$, which is due to the Rabi frequency equals zero at those points. It is known that without the pump field, the reflectivity is very low and the solid medium is completely opaque to the signal light near the resonance. When $\eta=0.1$, Ω_0 is not zero any more, in which the resonant absorption of the probe at the pump nodes no longer prevents the development of a photonic stop band [13,14]. Figure 6 shows that the gap width and κ'' within the gap become smaller than ones in Fig. 5(b) by reducing the two counterpropagating beams misalignment α along x, by which one can easily change in fact the spatial periodicity given by $a=(\lambda_c/2)/\cos(\alpha/2)$.

Finally, we consider the effect of incident angle θ of the probe (nonnormal incidence). The common theory we use comes from Ref. [19]. In Fig. 7 fixing all other parameters and only changing the angle of incidence we plot the imaginary part of the Bloch wave vector near the Brillouin zone boundary. From this figure, we can see that the position of PBG in a solid SW-EIT photonic crystal can be made relatively sensitive to the incident angle. When θ increases slightly from 0.35 to 1.96 mrad, on one hand, the width of PBG has a bigger change: from a larger value to a smaller value even to zero (PBG is barely created when $\theta=1.18$ mrad), and then to a larger value. On the other hand,
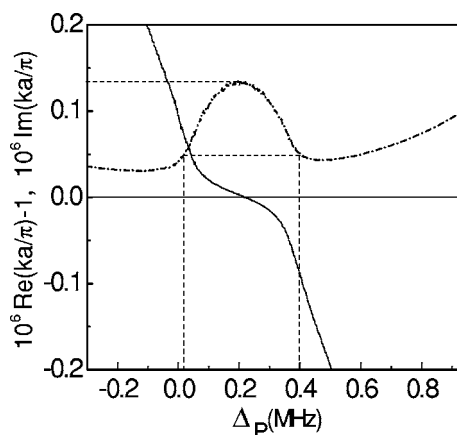
FIG. 6. Photonic band profile when a modified SW pump with $\alpha=0.506$ mrad is on. All other parameters are as in Fig. 5(b).

FIG. 7. Imaginary part of the Bloch wave vector near the Brillouin zone boundary corresponding to the normal incidence (thin solid *a*), and the small incident angle: 0.35 mrad (dash *b*), 1.18 mrad (solid *c*), 1.57 mrad (short dash *d*), and 1.96 mrad (dash dot *e*), respectively. All other parameters are as in Fig. 2.

the range where the probe propagation was forbidden changes from positive detunings to negative detunings (i.e., from long wavelength to short wavelength). By slightly tune θ can change the effect length between the coherent field and probe field, which in fact results in the change of the spatial periodicity a. According to papers [25,26] the center frequency of the forbidden band is sensitive to the gap width, so very small values of θ are enough to narrow and move the gap.

IV. CONCLUSION

Inhomogeneously broadened doped solids supporting electromagnetically induced transparency are viable materials where optically tunable photonic band gaps may be observed and results are shown for Pr: YSO [27]. We theoretically show that tuning the control beam Rabi frequency Ω_0 and the standing wave configuration (η, α, θ) may dynamically control the width, the size, and the position of the gaps.
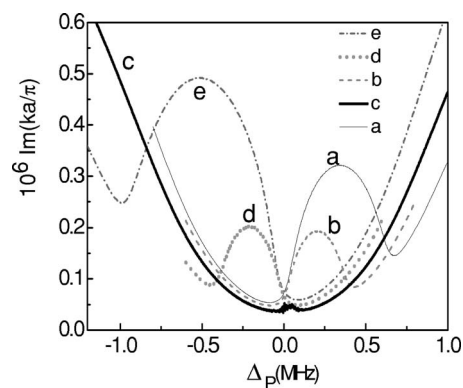
In comparison with the standard photonic crystals, we may get some explanation for results arising from these factors. Although we have chosen to discuss well-known experimental cases only, however many other inhomogeneously broadened doped solid are anticipated [17,28] to be amenable to the observation of electromagnetically induced transparency and, thus, to be useful for the realization of the all-optically photonic band gaps here considered. The accuracy and prompt tenability of these gap structures also may be employed for quantum light storage [29] and fast optical switching applications [16].

[1] K. J. Boller, A. Imamoglu, and S. E. Harris, Phys. Rev. Lett. **66**, 2593 (1991); S. E. Harris, J. E. Field, and A. Imamoglu, *ibid.* **64**, 1107 (1990); A. Kasapi, M. Jain, G. Y. Yin, and S. E. Harris, *ibid.* **74**, 2447 (1995); M. Xiao, Y. Q. Li, S. Z. Jin, and Gea-Banacloche Julio, *ibid.* **74**, 666 (1995); S. E. Harris, Phys. Today **50**(7), 36 (1997); M. O. Scully and M. S. Zubairy, *Quantum Optics* (Cambridge University Press, Cambridge, 1997).

[2] G. Alzetta, S. Gozzini, A. Lucchesini, S. Cartaleva, T. Karaulanov, C. Marinelli, and L. Moi, Phys. Rev. A **69**, 063815 (2004); A. Dantan and M. Pinard, *ibid.* **69**, 043810 (2004); Z. C. Zhuo, X. M. Su, and Y. S. Zhang, Phys. Lett. A **336**, 25 (2005).

[3] Y. Zhao, C. Wu, B. S. Ham, M. K. Kim, and E. Awad, Phys. Rev. Lett. **79**, 641 (1997); B. S. Ham, M. S. Shahriar, and R. P. Hemmer, Opt. Lett. **22**, 1138 (1997); K. Ichimura, K. Yamamoto, and N. Gemma, Phys. Rev. A **58**, 4116 (1998); A. V. Turukhin, V. S. Sudarshanam, M. S. Shahriar, J. A. Musser, B. S. Ham, and P. R. Hemmer, Phys. Rev. Lett. **88**, 023602 (2001); C. Wei and N. B. Manson, Phys. Rev. A **60**, 2540 (1999); J. J. Longdell, E. Fraval, M. J. Sellars, and N. B. Manson, Phys. Rev. Lett. **95**, 063601 (2005).

[4] B. S. Ham, P. R. Hemmer, and M. S. Shahriar, Opt. Commun. **144**, 227 (1997); B. S. Ham, M. S. Shahriar, M. K. Kim, and P. R. Hemmer, Opt. Lett. **22**, 1849 (1997); P. R. Hemmer, A. V. Turukhin, and M. S. Shahriar, Opt. Lett. **26**, 361 (2001).

[5] A. K. Patnaik, J. Q. Liang, and K. Hakuta, Phys. Rev. A **66**, 063808 (2002).

[6] E. A. Wilson, N. B. Manson, and C. Wei, Phys. Rev. A **67**, 023812 (2003).

[7] H. L. Xu, Z. W. Dai, and Z. K. Jiang, Phys. Lett. A **294**, 19 (2002).

[8] E. Kuznetsova, R. Kolesov, and O. Kocharovskaya, Phys. Rev. A **70**, 043801 (2004).

[9] C. Affolderbach, S. Knappe, R. Wynands, A. V. Talchenachev, and V. I. Yudin, Phys. Rev. A **65**, 043810 (2002).

[10] A. Andre and M. D. Lukin, Phys. Rev. Lett. **89**, 143602 (2002); M. Bajcsy, A. S. Zibrov, and M. D. Lukin, Nature (London) **426**, 638 (2003).

[11] M. Bajcsy, A. S. Zibrov, and M. D. Lukin, Nature (London) **426**, 638 (2003).

[12] X. M. Su and B. S. Ham, Phys. Rev. A **71**, 013821 (2005).

[13] M. Artoni, G. La Rocca, and F. Bassani, Phys. Rev. E **72**, 046604 (2005).

[14] M. Artoni and G. C. La Rocca, Phys. Rev. Lett. **96**, 073905 (2006).

[15] I. Friedler, G. Kurizki, and D. Petrosyan, Phys. Rev. A **71**, 023803 (2005).

[16] A. Andre, M. Bajcsy, A. S. Zibrov, and M. D. Lukin, Phys. Rev. Lett. **94**, 063902 (2005).

[17] E. Kuznetsova, O. Kocharovskaya, P. Hemmer, and M. O. Scully, Phys. Rev. A **66**, 063802 (2002); A. Javan, O. Kocharovskaya, Hwang Lee, and M. O. Scully, *ibid.* **66**, 013805 (2002).

[18] The use of Lorentzian lineshapes allows for the analytical results for χ as described in detail in Ref. [17]. Rather than reproducing those rather lengthy formulas here, we prefer to show χ for the cases of our interest in Fig. 2.

[19] M. Born and E. Wolf, *Principles of Optics*, 6th ed. (Cambridge University Press, Cambridge, 1980).

[20] F. Bassani and G. Pastori Parravicini, *Electronic States and Optical Transitions in Solids* (Pergamon Press, Oxford, 1975).

[21] A detailed treatment of coherently induced stop-bands in resonantly absorbing and inhomogeneously broadened doped crystals is given in Q. Y. He, Y. Xue, G. C. La Rocca, M. Artoni, J. H. Xu, and J. Y. Gao, Phys. Rev. B (to be published).

[22] Willem L. Vos, Mischa Megens, Carlos M. van Kats, and Peter Bösecke, J. Phys.: Condens. Matter **8**, 9503 (1996).

[23] X. D. Wang, K. Z. Yan, and F. Liu, J. Optoelectron., Laser **14**, 1063 (2003).

[24] M. Centini, M. Scalora, C. Sibilia, G. D'Aguanno, M. Bertolotti, M. J. Bloemer, and C. M. Bowden, J. Opt. A, Pure Appl. Opt. **2**, 121 (2000).

[25] A. Yariv and P. Yeh, *Optical Waves in Crystals* (Wiley InterScience, New York, 2003).

[26] E. L. Ivchenko, M. M. Voronov, M. V. Erementchouk, L. I. Deych, and A. A. Lisyansky, Phys. Rev. B **70**, 195106 (2004).

[27] In the same way, we also get the similar results for the case of nitrogen-vacancy (N-V) color centers in diamond (N-V diamond), too.

[28] M. Johnsson and K. Molmer, Phys. Rev. A **70**, 032320 (2004).

[29] M. Lukin, Rev. Mod. Phys. **75**, 457 (2003).